GBT Commissioning Memo:
Gregorian Focus Calibration at S-band:
empirical determination of optimum subreflector focus tracking in X and Y

Keywords: Low Frequency Gregorian Focus Tracking

F.Ghigo, R.Maddalena, D.Balser, G.Langston
March 23, 2001; revised: March 29, 2001

Introduction

Gravitational flexure of the GBT feed arm and main reflector causes significant motion of the focal point with respect to the subreflector as the antenna is moved in elevation. Estimates based on the structural model indicate that deviations of up to 20 cm or so are expected. (see Wells 1998, GBT Memo 183).

Of the 6 degrees of freedom of motions of the subreflector, we are concerned here with motion in only two of the axes: the "Y" axis, approximately towards and away from the nominal focus of the main 100-meter reflector, and the "X" axis, perpendicular to Y. (See figure 1) A third direction, the "Z" axis, is perpendicular to X and Y. These axes correspond to Xs, Ys, Zs in GBT memo 165 (Goldman, 1997). Adjustment of the “Z” axis is discussed in another memo.

Figure 1: Subreflector Axes

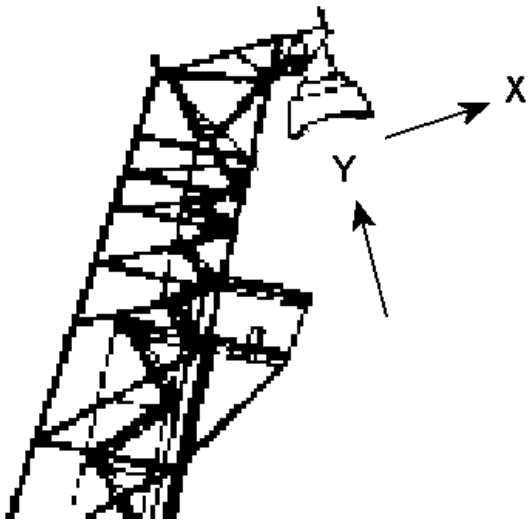

The subreflector "home" position was set mechanically so that at the rigging angle (50E) the optimum X and Y setting should both be near zero. Theoretically there should be no need to adjust the tilt at wavelengths greater than 0.5 cm. The Xs, Ys, Zs coordinate system was designed so that motion in Ys should produce minimal pointing error (Srikanth 1990: GBT Memo 49).

The purpose of these measurements is to determine empirically the deformations and to find the

optimum focus settings to correct for them.

Procedure

Measurements were made during February 23rd to March 6th of 2001 to determine the optimum X and Y focus settings as a function of elevation. Observing was at a frequency of 2.0 GHz with 80 MHz bandwidth in X linear polarization. The noise calibration was switched at 2 Hz rate. Total power detection was in the IF rack, and data was recorded with the DCR.

Tables 1 and 2 list the observation logs, and the derived optimum focus values. A focus scan sequence consisted of stepping the focus through its range. At each step a "cross" or "crossupdate" procedure was done to find the peak amplitude of the observed radio source. The steps in Y were from -10 inches to +10 inches (-254 to +254 mm) by steps of either 2.0 or 2.5 inches (51 or 64 mm). For X the steps went from -9 to +9 inches (-228.6 to +228.6 mm), also by steps of 2.0 or 2.5 inches.

A "cross" or "crossupdate" procedure consists of 4 scans: a scan across the source first in increasing RA, then back, followed by a scan in increasing DEC, then back. The local pointing corrections (LPCs) were adjusted before each set of 4 scans to put the source within about 2 arcmin of the correct position. After each set, new LPCs were calculated giving the improved pointing offsets. These corrections were determined by the on-line program "GO_point" by fitting a gaussian curve to each scan.

Figure 2 shows the 4-scan "cross" sequence for the source 3C219 with Y near the optimum value of 0 inches. The gaussian fitting finds the peak amplitude and half-power width for each scan. In the figure, the three numbers in a column at the left of each plot are the offset (arcminutes), fitted HPBW (arcminutes), and amplitude in units of Tcal.

Figure 2: "Cross" sequence of 4 scans: Y=0 in, elev=56E

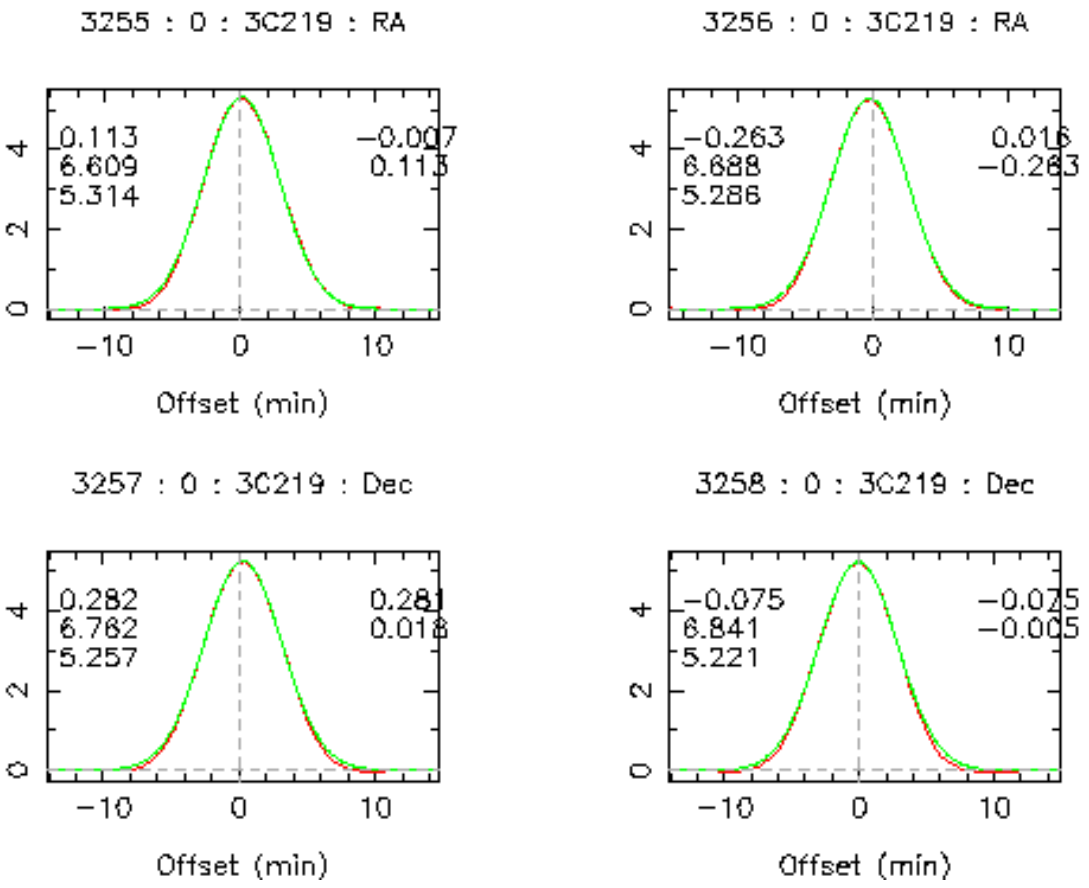

Figure 3 shows the same source with the Y focus near the extreme of its travel at Y = +10 inches. One can note that the maximum amplitude in this case is significantly less (2.9 as compared with 5.3), and the beam width larger (~8' as compared with 6.7' for the in-focus case).

Figure 3: "Cross" sequence of 4 scans: Y=+10in, elev=54E

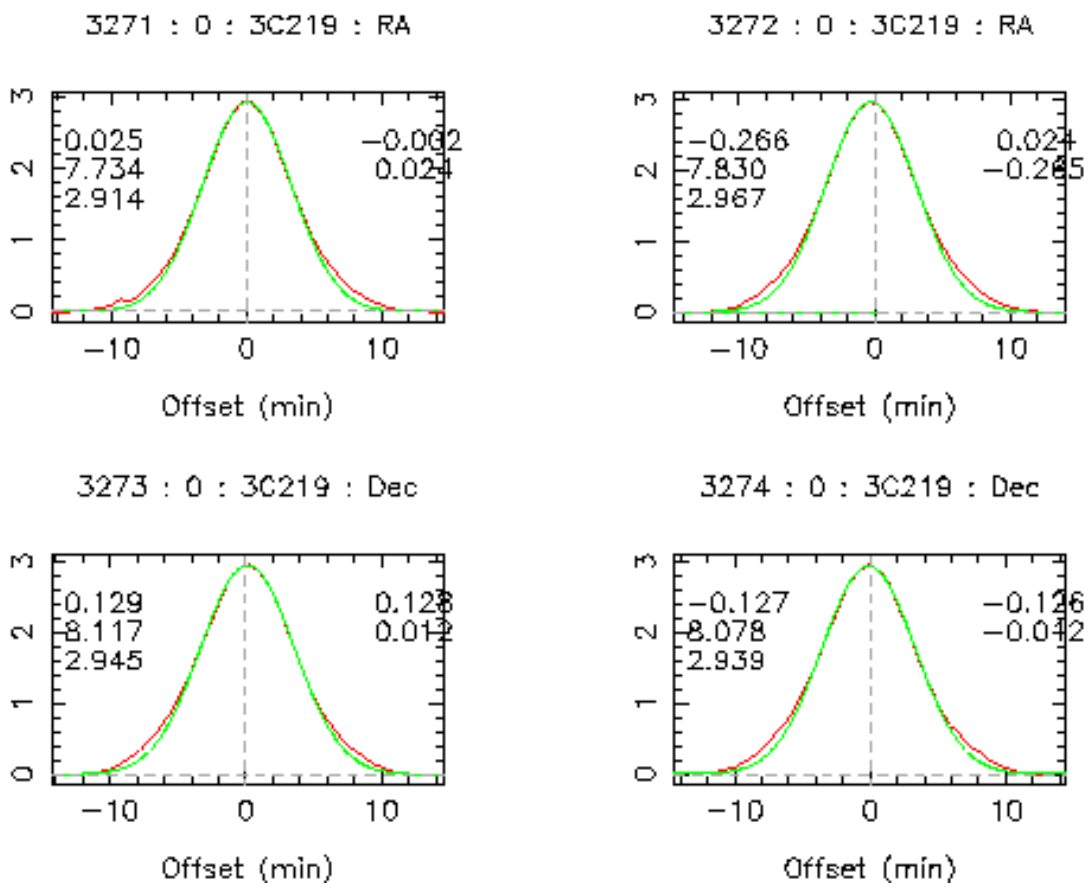

The average of the amplitudes of the two RA scans was compared with that of the DEC scans, and the higher of them was used as the amplitude associated with that focus setting.

In Figure 4, we plot the amplitude as found from each "cross" versus the Y-focus setting. A fifth-order polynomial was fit to the points and the focus value of the maximum was determined. The average elevation for the sequence of scans was calculated. The fitted Y-focus and average elevations are listed in Table 1 for all scan sequences.

Figure 4: Amplitude vs Y-focus setting and best fitting Y.

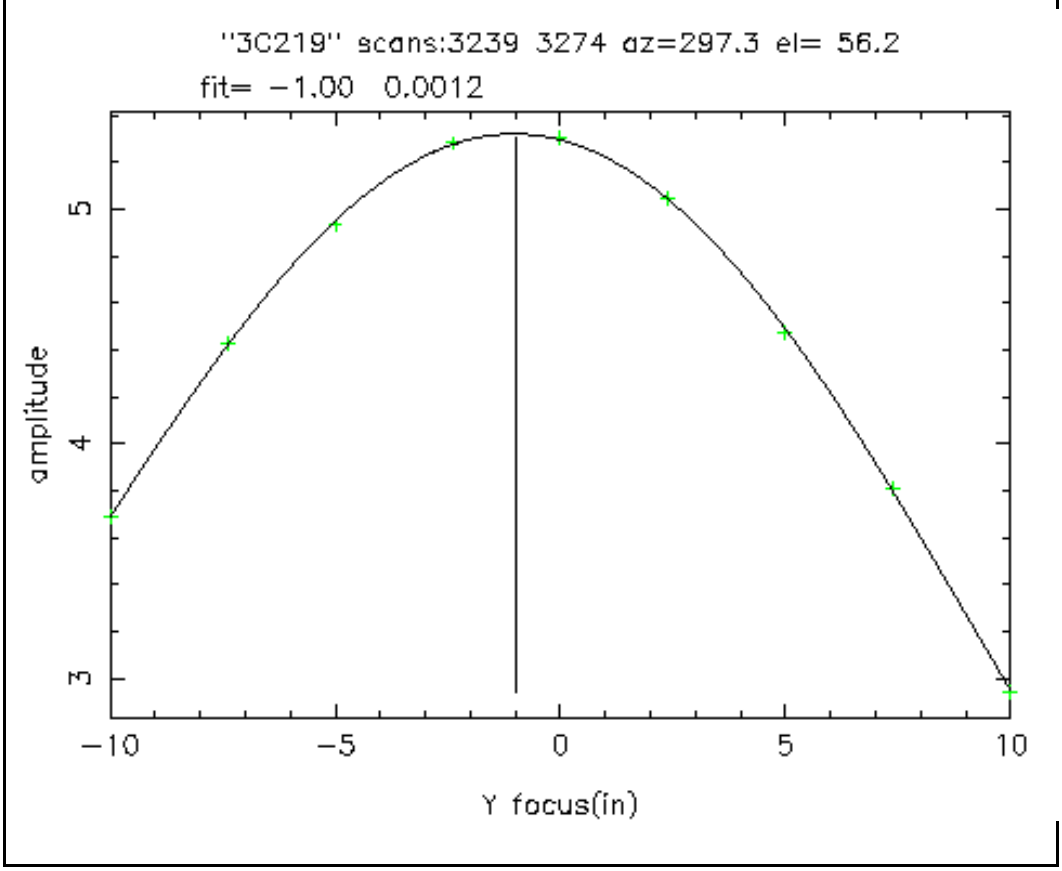

A similar procedure was followed for the X focus. Figure 5 shows an example of the amplitude vs X for one of the X-focus sequences. Table 2 lists the results for all of the X sequences.

Figure 5: Amplitude vs X-focus setting and best fitting X.

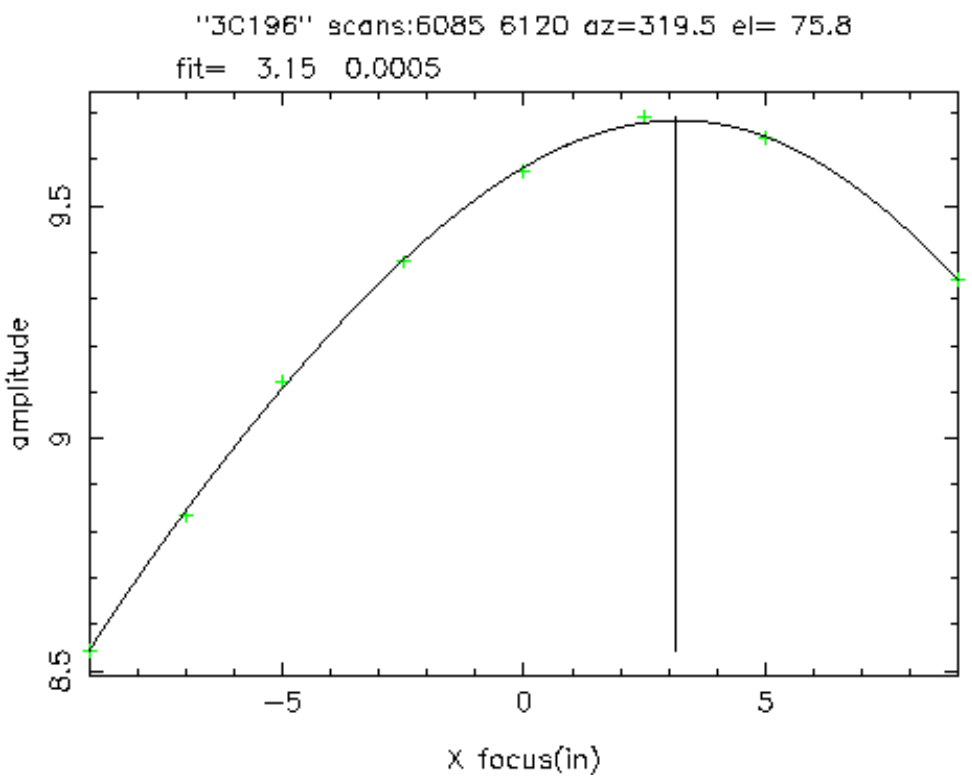

Results

For the Y-focus, the optimum Y values from Table 1 were plotted versus elevation, as shown in Figure 6. Some observations have been edited out due to presence of RFI, or poor fits.

Figure 6: Best fit Y vs Elevation (2-3GHz)

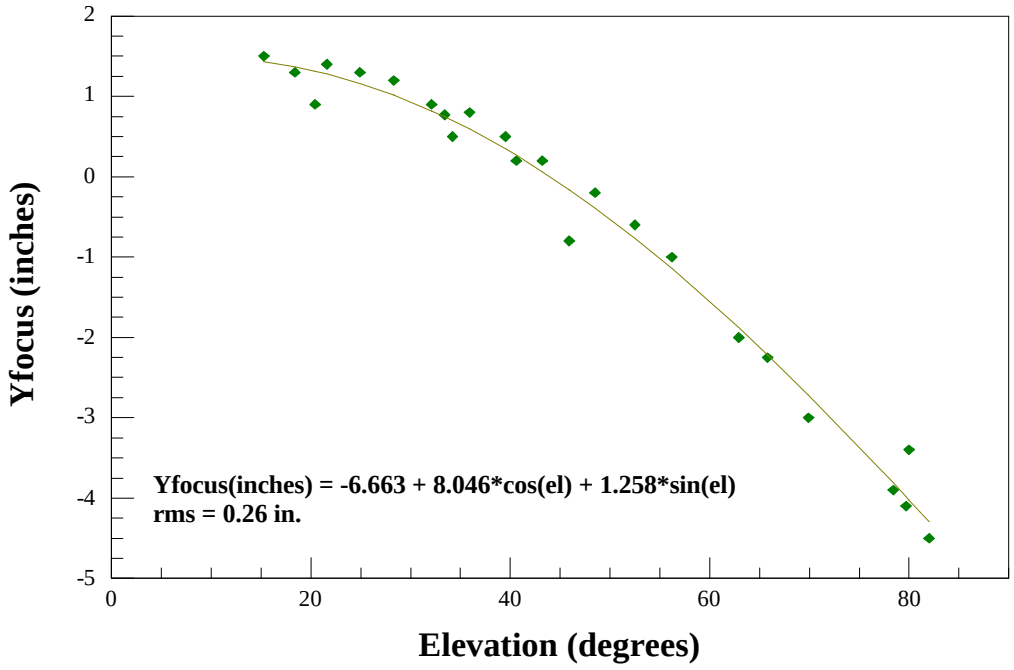

Likewise, Figure 7 shows the optimum X values from Table 2 plotted versus elevation.

Figure 7: Best fit X vs elevation (2-3GHz)

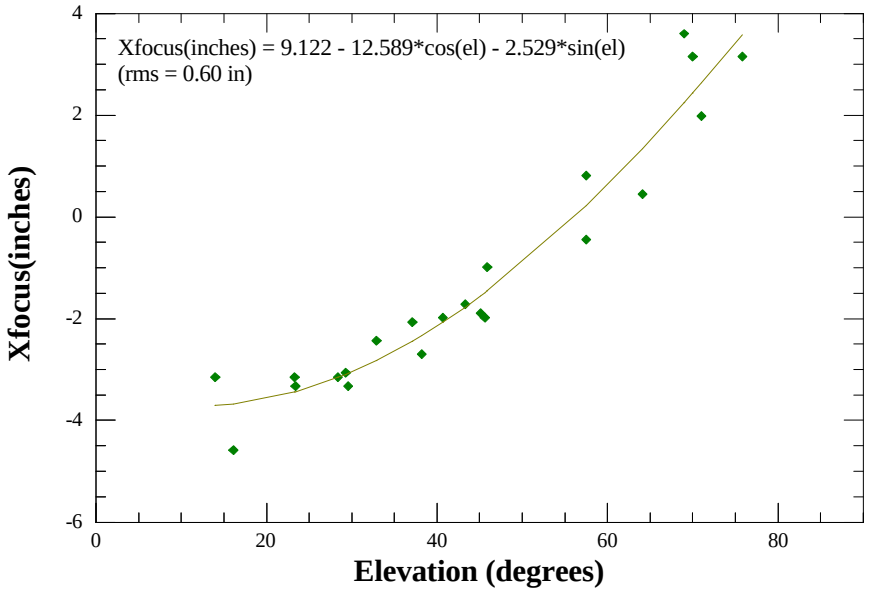

A curve of the form X = A + B*cos(el) + C*sin(el) was fit to the X focus data, and a curve of the same form to the Y focus data, with results as summarized in Table 3.

Table 3: Curve Fits to X and Y focus data		
fit = A + B*cos(el) + C*sin(el)		
Parameter	X-fit	Y-fit
A (inches)	9.122	-6.663
B (inches)	-12.589	8.046
C (inches)	-2.529	1.258
RMS (inches)	0.60	0.26

We expect that the optimum Y may shift slightly with observing frequency, because the effective phase center of the feed horn may be different at different frequencies. Likewise, there may be a shift in Y for different receivers.

We also note that ambient temperature changes will affect the calibration. These measurements should be repeated during the summer to evaluate the effect of temperature. These effects will become much more important at higher frequencies.

Finally, it is interesting to consider how well the mechanical alignment has succeeded. Our measurements show that the best fitting X and Y focus settings at the rigging angle of 50E are -0.91 and -0.53 inches, resp. Thus the mechanical alignment has put the home position of the subreflector within ~1 inch of the optimum position.

Table 1: Y-Focus Calibration Observations, GBT: 2-3GHz

Date-obs/ project	Source Name	scan numbers	Optimum Y(inches)	AZ (deg)	EL (deg)
23Feb2001 pnt_lowgreg_01	3C353	417 460	0.20	135.2	40.6
26Feb2001 pnt_lowgreg_02	3C161	642 669	0.77	227.4	33.4
	3C286	782 818	-3.40	141.0	80.0
	1337-1257	875 910	0.50	208.0	34.2
28Feb2001 pnt_lowgreg_04	3C295	1897 1932	-2.00	47.9	62.9
	1256-057	1941 1976	-0.80	177.0	45.9
	3C227	2029 2072	0.90	263.2	20.4
01Mar2001 pnt_lowgreg_05	3C219	3033 3068	-4.50	76.4	82.0
	3C196	3071 3110	-3.00	307.7	69.9
	3C196	3107 3142	-2.25	304.3	65.8
	3C219	3239 3274	-1.00	297.3	56.2
	3C219	3271 3306	-0.60	297.9	52.5
	3C219	3307 3342	-0.20	298.9	48.5
	3C219	3351 3386	0.20	300.6	43.2
	3C219	3383 3418	0.50	302.0	39.5
	3C219	3415 3450	0.80	303.6	35.9
	3C219	3447 3486	0.90	305.5	32.1
	3C219	3483 3518	1.20	307.6	28.3
	3C219	3515 3550	1.30	309.6	24.9
	3C219	3547 3582	1.40	311.8	21.6
	3C219	3579 3614	1.30	314.2	18.4
	3C219	3611 3646	1.50	316.8	15.3
08Mar2001 pnt_lowgreg_08	3C196	6008 6043	-3.90	27.0	78.4
	3C196	6044 6079	-4.10	309.1	79.7

Table 2: X-Focus Calibration Observations, GBT: 2-3GHz

Date-obs/ project	Source Name	scan numbers	Optimum X(inches)	AZ (deg)	EL (deg)
23Feb2001 pnt_lowgreg_01	3C353	373 404	-3.33	118.3	29.6
26Feb2001 pnt_lowgreg_02	3C161	710 737	-3.15	250.7	14.0
	3C286	746 773	3.15	106.1	70.0
	1337-1257	831 858	-2.70	190.5	38.2
27Feb2001 pnt_lowgreg_03	3C161	1085 1133	-3.06	233.6	29.3
	3C161	1134 1173	-3.33	241.1	23.4
	3C161	1182 1221	-4.59	248.7	16.1
	1256-0547	1270 1309	-1.98	171.8	45.6
	1256-0547	1310 1351	-0.99	182.2	45.9
	1256-0547	1352 1391	-1.89	192.9	45.1
	1256-0547	1393 1432	-1.71	203.0	43.3
	1256-0547	1433 1472	-1.98	212.1	40.7
	1256-0547	1473 1512	-2.07	220.7	37.1
	1256-0547	1513 1552	-2.43	228.4	32.9
	1256-0547	1553 1594	-3.15	235.0	28.4
	1256-0547	1595 1634	-3.15	241.3	23.3
28Feb2001 pnt_lowgreg_03	1008+075	1789 1824	0.81	158.5	57.5
01Mar2001 pnt_lowgreg_04	3C219	3151 3190	3.60	299.3	69.0
08Mar2001 pnt_lowgreg_08	3C196	6085 6120	3.15	319.5	75.8
	3C196	6125 6162	1.98	309.1	71.0
	3C196	6175 6210	0.45	303.5	64.1
	3C196	6215 6250	-0.45	302.1	57.5